

Molecular dynamics simulations of mutated *Mycobacterium tuberculosis* L-alanine dehydrogenase to illuminate the role of key residues



Baoping Ling^{a,*}, Siwei Bi^a, Min Sun^a, Zhihong Jing^a, Xiaoping Li^a, Rui Zhang^b

^a School of Chemistry and Chemical Engineering, Qufu Normal University, Qufu, Shandong 273165, China

^b Shandong Key Laboratory of Edible Mushroom Technology, School of Agriculture, Ludong University, Yantai, Shandong 264025, China

ARTICLE INFO

Article history:

Accepted 25 March 2014

Available online 4 April 2014

Keywords:

Mycobacterium tuberculosis

L-Alanine dehydrogenase

Essential dynamics analysis

Molecular dynamics simulations

Mutated residues

ABSTRACT

L-Alanine dehydrogenase from *Mycobacterium tuberculosis* (L-MtAlaDH) catalyzes the NADH-dependent interconversion of L-alanine and pyruvate, and it is considered to be a potential target for the treatment of tuberculosis. The experiment has verified that amino acid replacement of the conserved active-site residues which have strong stability and no great changes in biological evolutionary process, such as His96 and Asp270, could lead to inactive mutants [Ågren et al., J. Mol. Biol. 377 (2008) 1161–1173]. However, the role of these conserved residues in catalytic reaction still remains unclear. Based on the crystal structures, a series of mutant structures were constructed to investigate the role of the conserved residues in enzymatic reaction by using molecular dynamics simulations. The results show that whatever the conserved residues were mutated, the protein can still convert its conformation from open state to closed state as long as NADH is present in active site. Asp270 maintains the stability of nicotinamide ring and ribose of NADH through hydrogen bond interactions, and His96 is helpful to convert the protein conformation by interactions with Gln271, whereas, they would lead to the structural rearrangement in active site and lose the catalytic activity when they were mutated. Additionally, we deduce that Met301 plays a major role in catalytic reaction due to fixing the nicotinamide ring of NADH to prevent its rotation, and we propose that Met301 would be mutated to the hydrophobic residue with large steric hindrance in side chain to test the activity of the protein in future experiment.

© 2014 Elsevier Inc. All rights reserved.

1. Introduction

Tuberculosis (TB) is an infectious bacterial disease caused by *Mycobacterium tuberculosis*, which affects and persists in the lungs of infected individuals for decades by switching to a dormant or latent phases, therefore, it poses a major threat to human health [1]. Each year, new active cases increase by 9 million following 2 million deaths as a result (http://www.webtb.org/death_rate.php). Treatment of tuberculosis is complicated due to the emergence of multidrug-resistant and extensively drug-resistant strains of *M. tuberculosis* [2]. It may be difficult to control the number of infected individuals by TB without more powerful drugs, accordingly, the need for new antimicrobial drugs to expand the scope of TB treatment is urgently acute [3].

L-Alanine dehydrogenase (L-AlaDH) is known to be required for *Bacillus subtilis* which is one of species from *Bacillus* to utilize alanine as a sole carbon and nitrogen source during the normal sporulation [4]. L-AlaDH catalyzes the NADH-dependent reversible conversion of pyruvate and ammonia to L-alanine [5]. Since the crystal structure of human L-AlaDH has not been solved, L-AlaDH from *M. tuberculosis* (L-MtAlaDH) was used in this study, which is a secretory antigen associated with bacterial persistence during infection [6]. When the organisms were in the persistent phase, expression of the gene *ald* encoding for the enzyme L-AlaDH is up-regulated, which results in the increase of the enzymatic production and activity in *M. tuberculosis* [7], therefore, L-MtAlaDH is proposed to be a potential target for pathogen control by antibacterial drugs [8]. Crystallographic structures show that L-MtAlaDH is composed of a substrate-binding domain and a NAD-binding domain, which are connected by two α -helices [6,8], as shown in Fig. 1. The substrate-binding domain rotated by 16° toward the NAD-binding domain upon NAD binding to make them more accessible [6,8]. However, L-MtAlaDH completely lost its catalytic activity when the conserved residues such as His96 and Asp270

* Corresponding author at: School of Chemistry and Chemical Engineering, Qufu Normal University, West Jingxuan Road No.57, Qufu, Shandong 273165, China.
Tel.: +86 537 4456200.

E-mail address: baopingling@mail.qfnu.edu.cn (B. Ling).

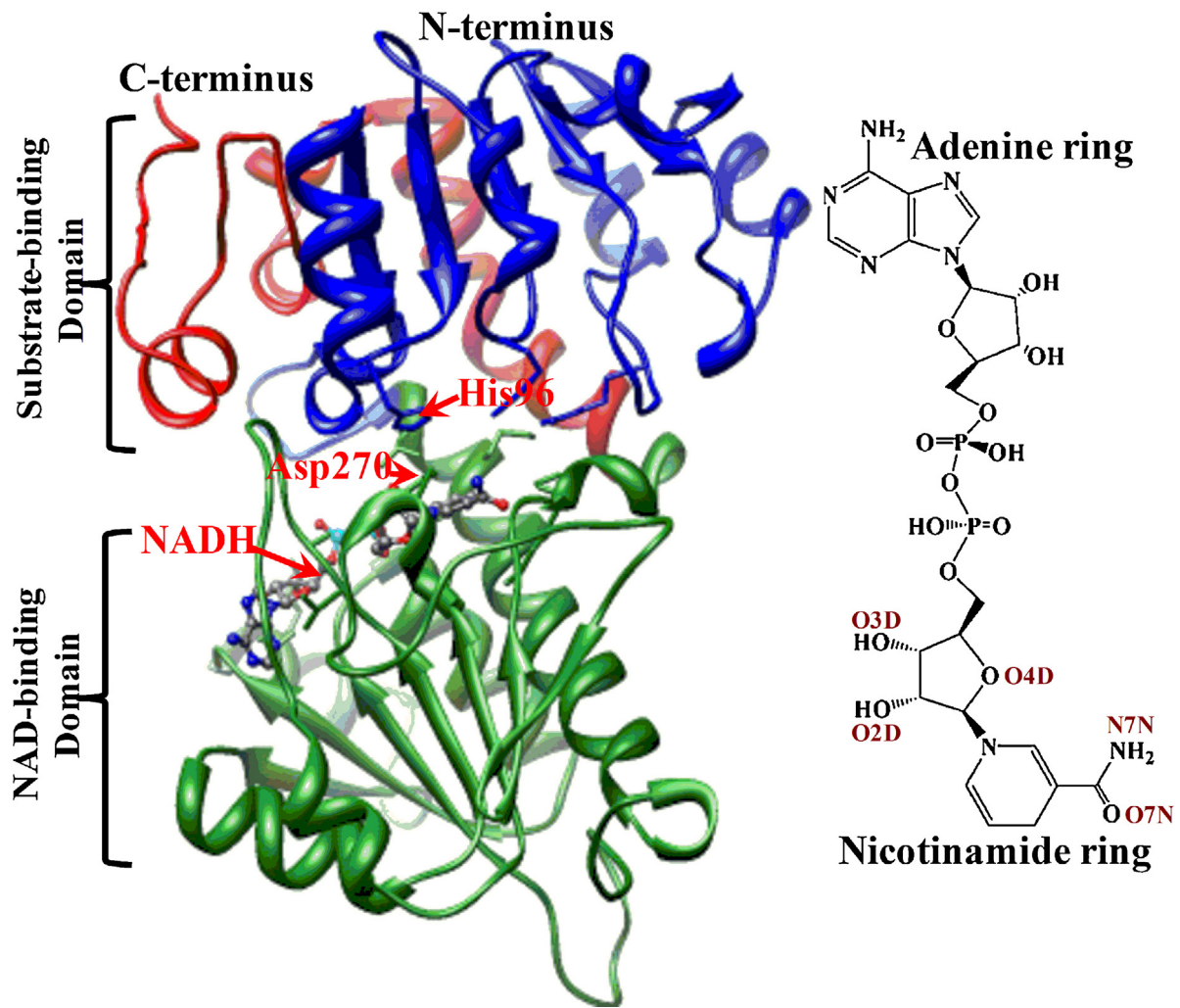


Fig. 1. Crystal structure of L-MtAlaDH bound NADH coenzyme (PDB code: 2VOJ) and the geometry structure of NADH. The protein is shown in ribbon and NADH in ball and stick model. C-terminus and N-terminus are colored in red and blue, respectively. Substrate-binding domain is represented by red and blue ribbon, and NAD-binding domain is shown in green ribbon.

were mutated, which play an essential role in enzymatic reaction in active site, and have strong stability and no great changes in biological evolutionary process. Ågen et al. have proposed possible catalytic mechanism as shown in Scheme 1, and identified the conserved active-site residues as potential catalysts in the reaction by site-directed mutagenesis [8]. The experimental results revealed that amino acid replacement by mutation led to inactive mutants, however, no obvious structural difference was observed in the position of active-site residue or the bound NADH [8]. Up to now, the role of the conserved residues in the catalytic reaction still remains unclear. The present work aims to study the role of key residues in the wild type protein by mutation, therefore, based on the crystal structures, a series of models with mutations were generated to perform molecular dynamics (MD) simulations to investigate the effect of conserved residues on the structure and activity of L-MtAlaDH.

2. Methods

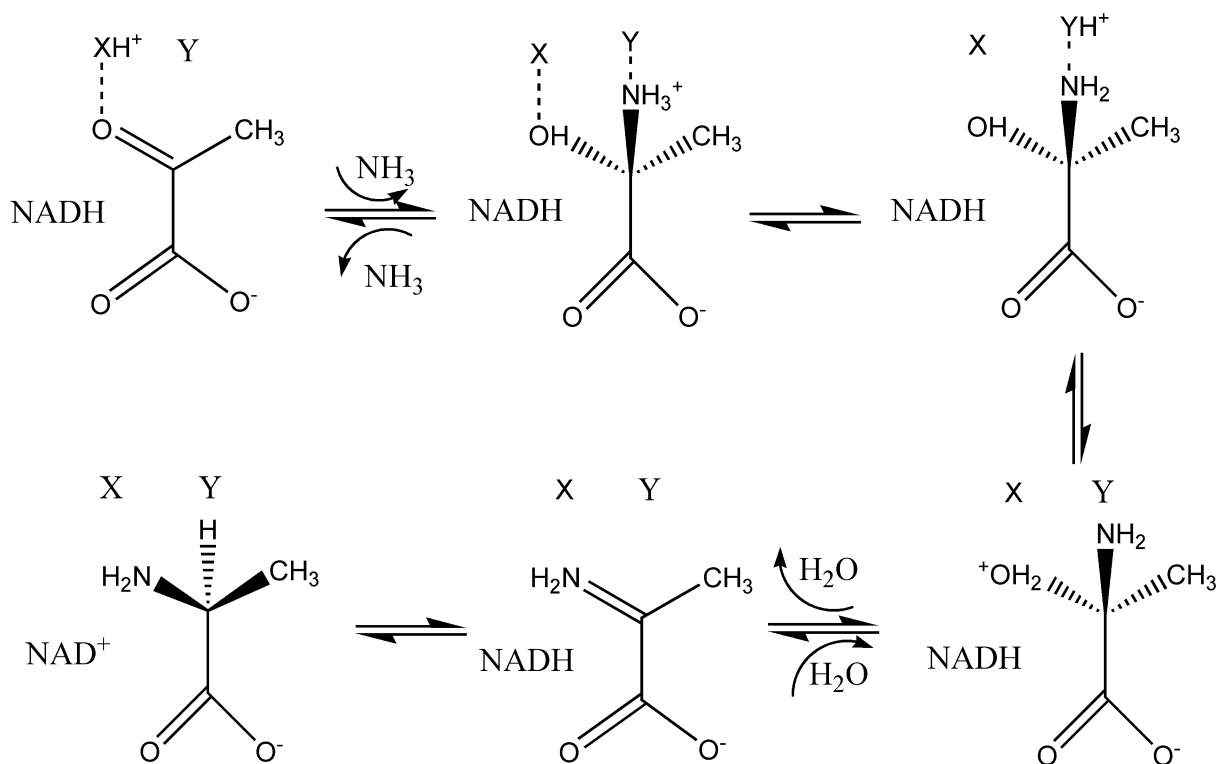
2.1. Preparation of structures

The X-ray crystal structures of L-MtAlaDH, downloaded from the Brookhaven Protein Data Bank (<http://www.rcsb.org/pdb>), were

used for preparing the initial structures for MD simulations. The crystal structures used in the present work and their abbreviations are listed in Table 1, wherein, MD simulations of three systems WT_apo, WT_holo and WT_hybrid were performed in our previous study [9]. In this work, to explore the role of conserved residues in active site, such as His 96 and Asp 270, a series of mutant structures were generated based on the crystal structures. This work refers to WT as wild type, SM as single mutation and DM as double mutation for L-MtAlaDH, respectively. Apo refers to L-MtAlaDH in open state without coenzyme NADH, holo represents the NADH bound to enzyme in closed state, and hybrid reflects the NADH bound to enzyme in open state. The mutated residues were created with VMD 1.8.6 program [10].

2.2. Parameter setup for MD simulations

Based on our previous MD simulations [9], several structures with mutations were subjected to MD simulations. Each structure was solvated in the simple point charge (SPC) water molecules [11] in a cubic box with periodic boundary conditions, and several Na⁺ ions were added to maintain charge neutrality by randomly replacing water molecules. The size of each system is also listed in Table 1. The temperature was kept constant at 300 K by coupling



Scheme 1. Possible catalytic mechanism of the reversible conversion of pyruvate and ammonia to L-alanine catalyzed by L-AlaDH, adapted from reference 8. X and Y are two groups on enzyme. The nicotinamide ring of NADH is below the substrate, and hydride transfer results in the formation of L-alanine.

to a modified Berendsen thermostat [12] with a coupling time of 0.1 ps. The pressure was kept at 1 atm by coupling to an isotropic scaling with a relaxation time constant of 2.0 ps. The LINCS algorithm [13] was used to constrain bond lengths involving hydrogen atoms. The particle mesh Ewald (PME) method [14] with a 1.0 nm cutoff was applied for calculating long-range electrostatic interactions. Nonbonded interactions were calculated with a 1.4 nm cutoff. NADH parameters were generated in PROGRG server [15] using the GROMOS96 force field [16]. The standard protonation states were assigned by default for all residues in pdb2gmx module, and His was assigned to deprotonated state by default. All simulations were carried out with software package GROMACS 4.0.4 [17,18] using the GROMOS96 force field [16].

Each molecular system was minimized for 10,000 steepest-descent steps. Subsequently, the systems were equilibrated for 100 ps under constant volume (NVT) and constant pressure (NPT) conditions, respectively, during which movements of heavy atoms of protein were restrained harmonically with a force constant of 1000 kJ mol⁻¹ nm⁻², while other atoms were relaxed [19–22]. Finally, the systems were subjected to 30 ns MD simulations

allowing the movements of all atoms [23,24], and the trajectories were saved at an interval of 10 ps for analysis. All protein structures were plotted with Chimera [25].

2.3. Essential dynamics analysis

Essential dynamics (ED) analysis, also called principle component analysis (PCA), is utilized to find correlated motions of protein through the eigenvectors obtained from diagonalization of the mass-weighted covariance matrix of atomic positional functions. It can transform the original space of correlated variables into a reduced space of independent variable, i.e., the principle component [26]. In other words, it can transform the original high-dimensional representation of protein motions into a low-dimensional one which reveals the prominent motional mode of protein [26,27]. Its principle has been described in detail elsewhere [28–30]. In the present study, only the eigenvectors with large eigenvalues were used to describe the protein motions, and ED analysis was performed using the GROMACS suite of programs [17,18].

Table 1
Crystal structures referred to in this work and their abbreviations.

Abbreviation	Residues before mutation	Residues after mutation	Na ⁺ number	Total atoms	PDB code	Resolution (Å)
WT_apo ^a	–	–	7	75,195	2voe	2.6
WT_holo ^a	–	–	8	72,299	2voj	2.6
WT_hybrid ^a	–	–	8	68,507	2vhw	2.0
SM1_hybrid ^b	Asp270	Asn270	6	66,197	2vhw	2.0
SM2_crystal ^b	Asp270	Asn270	7	65,424	2vhv	2.8
SM3_hybrid ^b	His96	Ala96	7	66,191	2vhw	2.0
DM_hybrid ^c	Asp270, His96	Asn270, Ala96	7	67,641	2vhw	2.0
DM_holo ^c	Asp270, His96	Asn270, Ala96	7	67,633	2voj	2.6

^a WT refers to wild type L-MtAlaDH.

^b SM refers to L-MtAlaDH with a single mutated residue.

^c DM refers to L-MtAlaDH with two mutated residues.

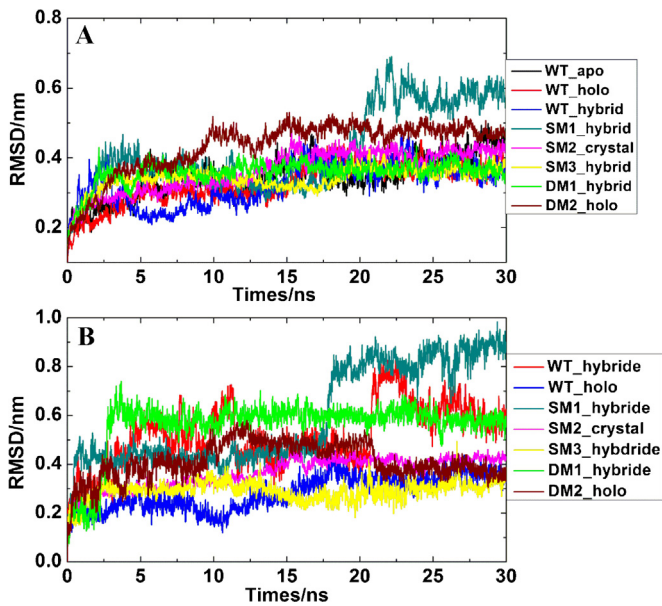


Fig. 2. Time evolutions of RMSDs from different systems during entire 30 ns MD simulations. (A) RMSDs of protein (protein after least-squares fit to protein); (B) RMSDs of ligand (ligand after least-squares fit to protein).

3. Results and discussions

3.1. Equilibrium dynamics from MD simulations

To confirm the equilibration of 30 ns MD simulations, we calculated the root-mean square deviations (RMSD) of C α atoms against an energy-minimized structure for each system, and the data were shown in Fig. 2. From Fig. 2A, it can be seen that RMSD values of protein (protein after least-squares fit to protein) for most of systems are maintained in the range of 0.3–0.4 nm from 3 ns, and these values are slightly higher because the proteins change their conformations upon NADH binding. However, RMSD values of SM1_hybrid and DM2_holo systems are larger than 0.5 nm, especially for SM1_hybrid (over 0.6 nm), which may be caused by

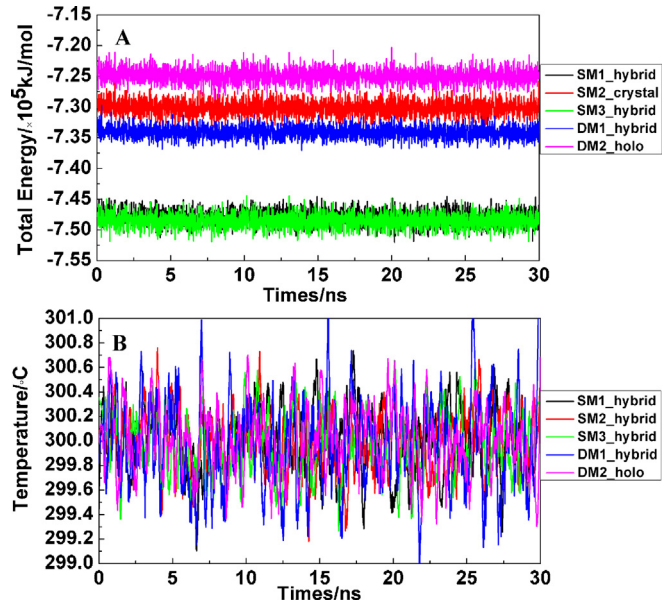


Fig. 4. Total energies (A) and temperature (B) as a function of time for each system during 30 ns MD trajectories.

the instability of coenzyme NADH. These results are consistent with RMSD values of ligand (ligand after least-squares fit to protein) in Fig. 2B. Based on our previous study [9], the adenine ring of NADH is unstable because it interacts with the surrounding residues in binding pocket through weak hydrophobic interactions rather than strong hydrogen bonds, which leads to the dramatic structural rearrangement of protein and large RMSD values. For SM1_hybrid system, the superimposition of average structures from 3–17 ns to 22–30 ns is displayed in Fig. 3. It is obvious that the dramatic structural changes have taken place in the substrate-binding domain due to the movement of adenine ring of NADH, therefore, 0–17 ns trajectories of SM1_hybrid system were used to analyze in the present study. In addition, the total energy and temperature are calculated for each system, as shown in Fig. 4. It is clear that the total energy oscillates around the average energy,

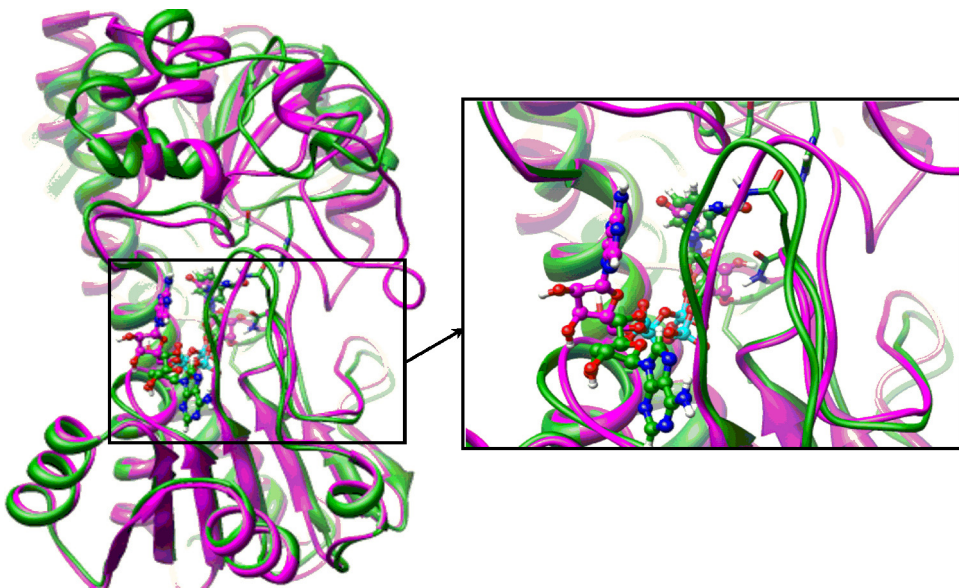


Fig. 3. Superimposition of the average structures from 3 to 17 (green) and 22–30 (magenta) ns trajectories for SM1_hybrid system. The protein is shown in ribbon and NADH in ball and stick model. The residues interacting with NADH are represented in stick. (For interpretation of the references to color in this figure legend, the reader is referred to the web version of this article.)

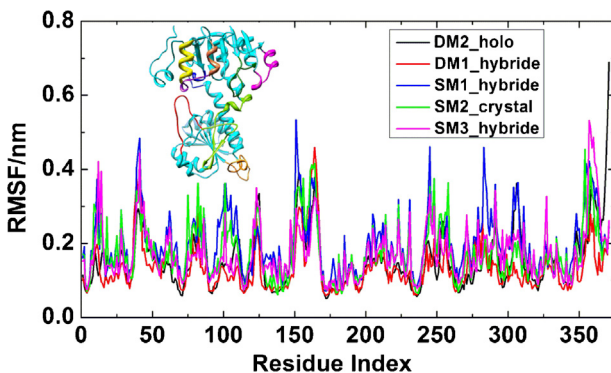


Fig. 5. Root mean square fluctuation of each residue from different systems during 30 ns simulations. The inset shows the high flexible regions according to RMSF values. Residues 6–20, dark green; 40–53, magenta; 79–85 (α 1), coral; 94–100 (loop1), purple; 101–110 (α 2), yellow; 117–127 (loop2), blue; 150–169, orange and 238–251 (loop3), red; 280–308, chartreuse. (For interpretation of the references to color in this figure legend, the reader is referred to the web version of this article.)

and the temperature also fluctuates at 300 K. Taken altogether, each system basically reaches equilibrium after 3 ns.

Comparative analysis of the root mean square fluctuations (RMSF) of each residue is shown in Fig. 5. It is obvious that the flexible regions of protein are basically similar for each system, and the regions with higher flexibility are two α -helices (residues 79–85 and 101–110) and three loops (residues 94–100, 117–127 and 238–251). In addition, except for C-terminal residues, despite some regions, such as residues 6–20, 40–53, 150–169 and 280–308, exhibit high mobility, they are not considered significant for the study since they are far from the active site. Moreover, RMSF values of DM1_hybrid and DM2_holo systems are lower than those of SM1_hybrid, SM2_crystal and SM3_hybrid systems, which shows the protein structure with double mutation is more stable than that with single mutation.

3.2. ED analysis

Since protein has high dimensionality, it is rather difficult to identify the biological important motions. Therefore, the concerted motions of protein were determined by ED analysis. Fig. 6A shows the relative contribution of the different eigenvectors to the overall motion of protein. It is clear that the bulk of dynamics can be described by a small number of eigenvectors. Moreover, the inset shows the first 10 eigenvectors contributed to the total variance account for above 80%, especially for SM1_hybrid system $\sim 90\%$. The first eigenvector provides great contribution, representing $\sim 40\%$ of the total mean-square fluctuations, and $\sim 60\%$ in SM1_hybrid system. Hence, the first 10 eigenvectors are sufficient to use to assess the similarity and concerted motions of protein.

To compare regions sampled by the essential motions from different systems, two-dimensional projections onto the plane defined by the first two eigenvectors are given in Fig. 6B, which used a single trajectory to generate a conformational space, and then all other trajectories were projected on this space. Although a considerable overlap was observed, there are notable differences in fluctuations. The conformational space of DM1_hybrid overlapped well with that of SM3_hybrid, and the spaces of SM1_hybrid and DM2_holo distribute widely, which suggests that they have large conformational space, and this is in accordance with the result of RMSD. Especially for SM1_hybrid, from either the eigenvalue profiles or two-dimensional projections, one can see that the D270N mutation brings serious impact on the motion and conformational space of protein. Additionally, projections of each system onto the first and second eigenvectors with simulation time are given in

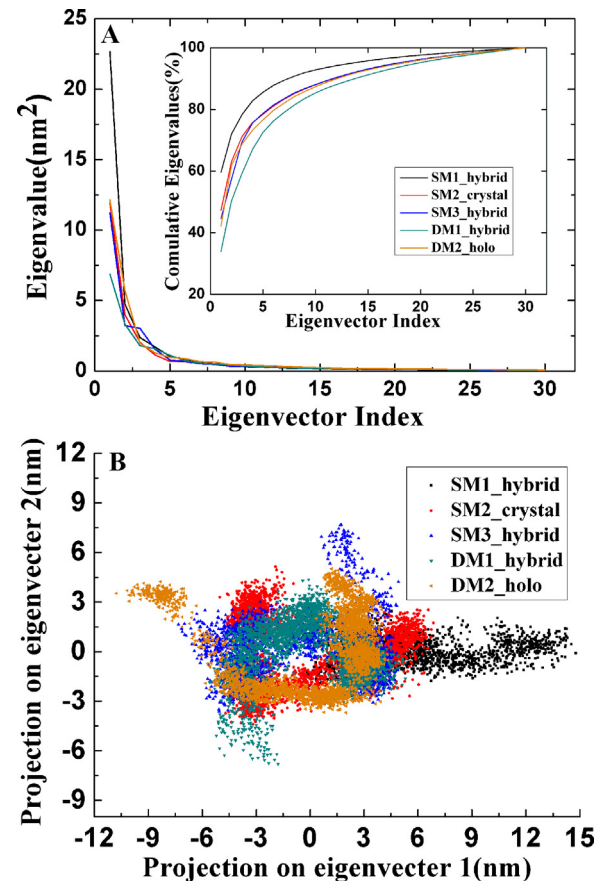


Fig. 6. Eigenvalue profile and comparative sampling of essential motions. These data derived from ED analysis of the 30 ns simulation trajectories, except for SM1_hybrid trajectory from 0–17 ns because of instability of adenine ring of NADH. (A) Eigenvalues of the first 30 eigenvectors, and the inset shows the cumulative contribution of these eigenvectors. (B) Two-dimensional projection of backbone atomic trajectories along the first two eigenvectors.

Fig. 7. In Fig. 7A, one can see that the eigenvalues of the first eigenvector from SM1_hybrid, SM2_crystal and SM3_crystal three systems decrease with time and keep stable after 20 ns. In particular, SM1_hybrid fluctuates with higher values. However, the values of DM1_hybrid and DM2_holo systems increase and stabilize after 15 ns. These results indicate that the proteins convert their conformations from open to closed state through closing motion for three single mutation systems, but two systems with double mutation change their conformations through opening motions. However, Fig. 7B shows that the twisting motion of DM1_hybrid system is significant and different from other systems. Overall, the protein still changes its conformation from open to closed state for DM1_hybrid. Therefore, the mutation of residues strongly affects the protein opening/closing and twisting motions. These results show that the mutated residues and protein state severely affect the conformational space and concerted motions of protein.

3.3. Role of His96 and Asp270 in active site of wild type L-MtAlaDH

Crystal structures resolved by Ågren et al. [8] and Tripathi et al. [6] clearly demonstrated that Asp270 and His96 were suitably positioned at the distance of 3 Å to the pyruvate carbonyl oxygen atom. Furthermore, a hydrogen bond between Met301 and the nicotinamide ring of NADH was formed, and the bifurcated hydrogen bond between the ribose of NADH and Asp270 was observed. In addition, a hydrogen bond between the nicotinamide ring of NADH and

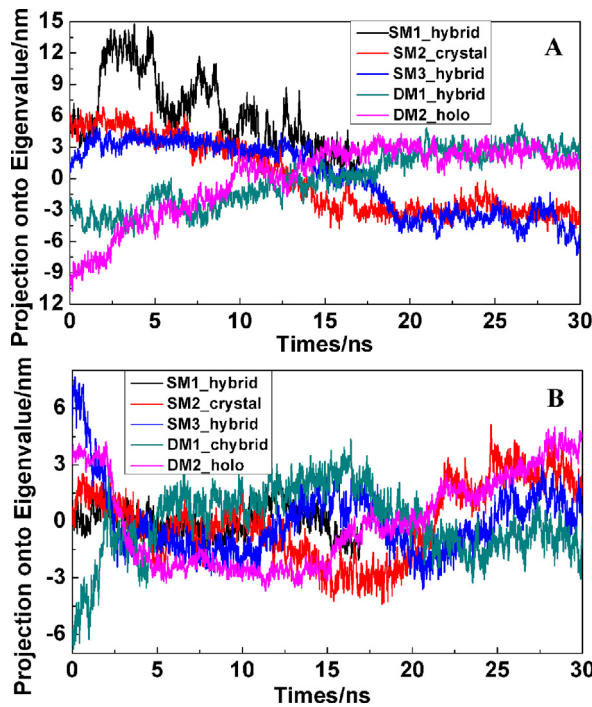


Fig. 7. Projections of the backbone atom trajectory onto the first (A) and second (B) eigenvectors as a function of time. For SM1_hybrid system, 0–17 ns trajectories are used to analyze.

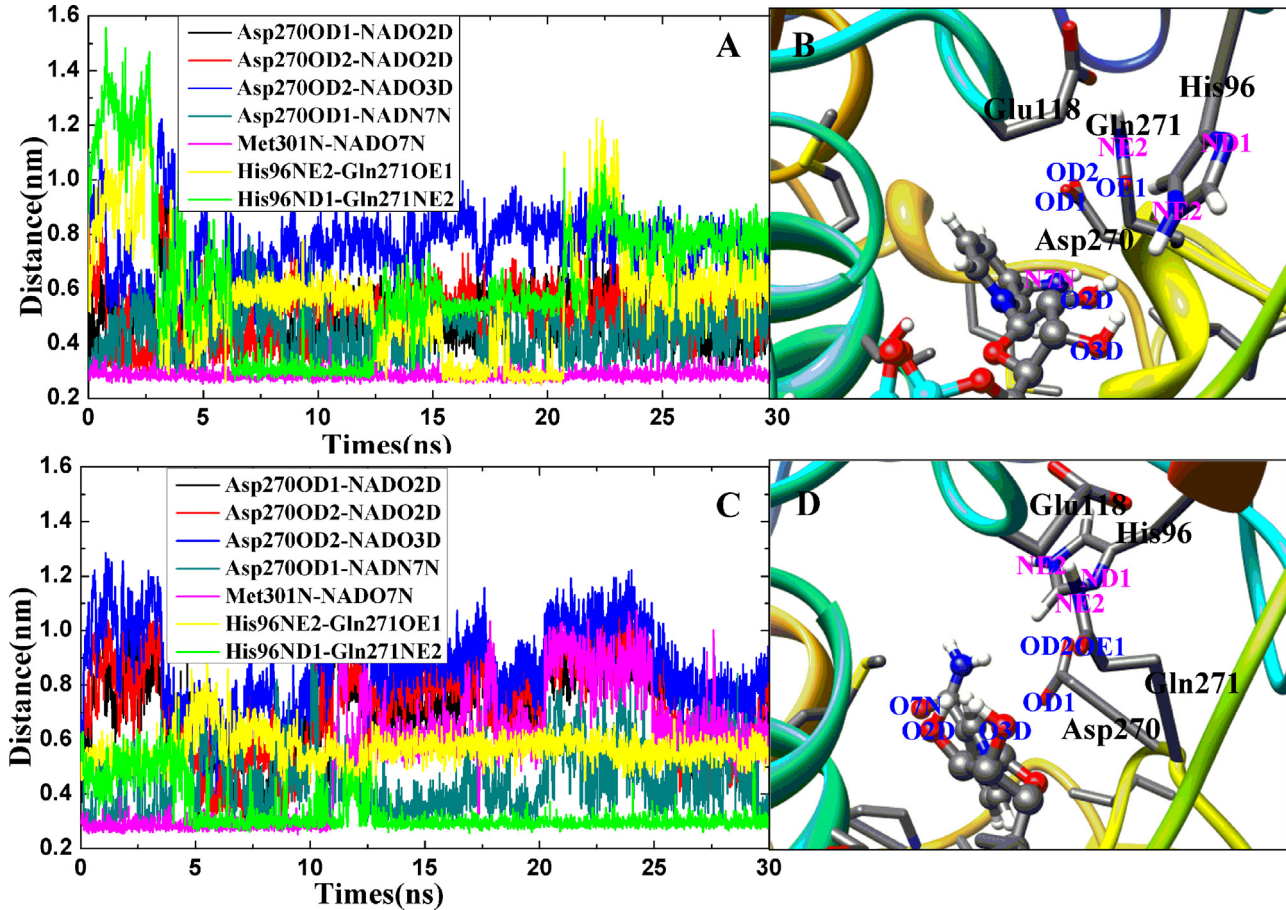


Fig. 8. Distance profiles between two heavy atoms of WT_hybrid (A) and WT_holo (C) systems. Average structures from 15 to 30 ns MD trajectories of WT_hybrid (B) and WT_holo (D) systems.

Asp270 was also found. Accordingly, these hydrogen bonds were analyzed to investigate the role of residues Asp270 and His96 in catalysis.

Fig. 8 gives the time courses of distance between heavy atoms of WT_hybrid and WT_holo systems, and their average structures from 15 ns to 30 ns MD trajectories. For WT_hybrid system, **Fig. 8A** depicts that the distance between OD1 of Asp270 and N7N of NADH fluctuates at 0.4 nm, but other atomic distances between two oxygen atoms of Asp270 and two oxygen atoms in the ribose of NADH fluctuate in the range of 0.4–0.8 nm. In addition, the distance between ND1 of His96 and NE2 of Gln271 decreases from 1.4 nm to 0.3 nm before 12 ns, which suggests that the protein changes its conformation from open state to closed state and forms a strong hydrogen bond which is disrupted after 12 ns. The superimposition of crystal structure and average structures from MD trajectories in **Fig. 9B** and D also demonstrates the substrate-binding domain moves down to close the NAD-binding domain during the MD simulations, and the inset in **Fig. 9C** shows that the hydrogen bond disappears owing to the displacement of His96 with the downward movement of substrate-binding domain. The inset in **Fig. 9A** further verifies the adenine ring is not stable and moves up to cause the movement of loop. Whereas, a strong hydrogen bond between N of Met301 and O7N of NADH is formed and always stabilizes at 0.3 nm. Therefore, we deduce that Met301 plays a critical role in maintaining the stability of nicotinamide ring of NADH, however, this has not been demonstrated by experiment. Based on this result, we propose that Met301 in WT protein will be mutated to the hydrophobic residue with large steric hindrance in side chain

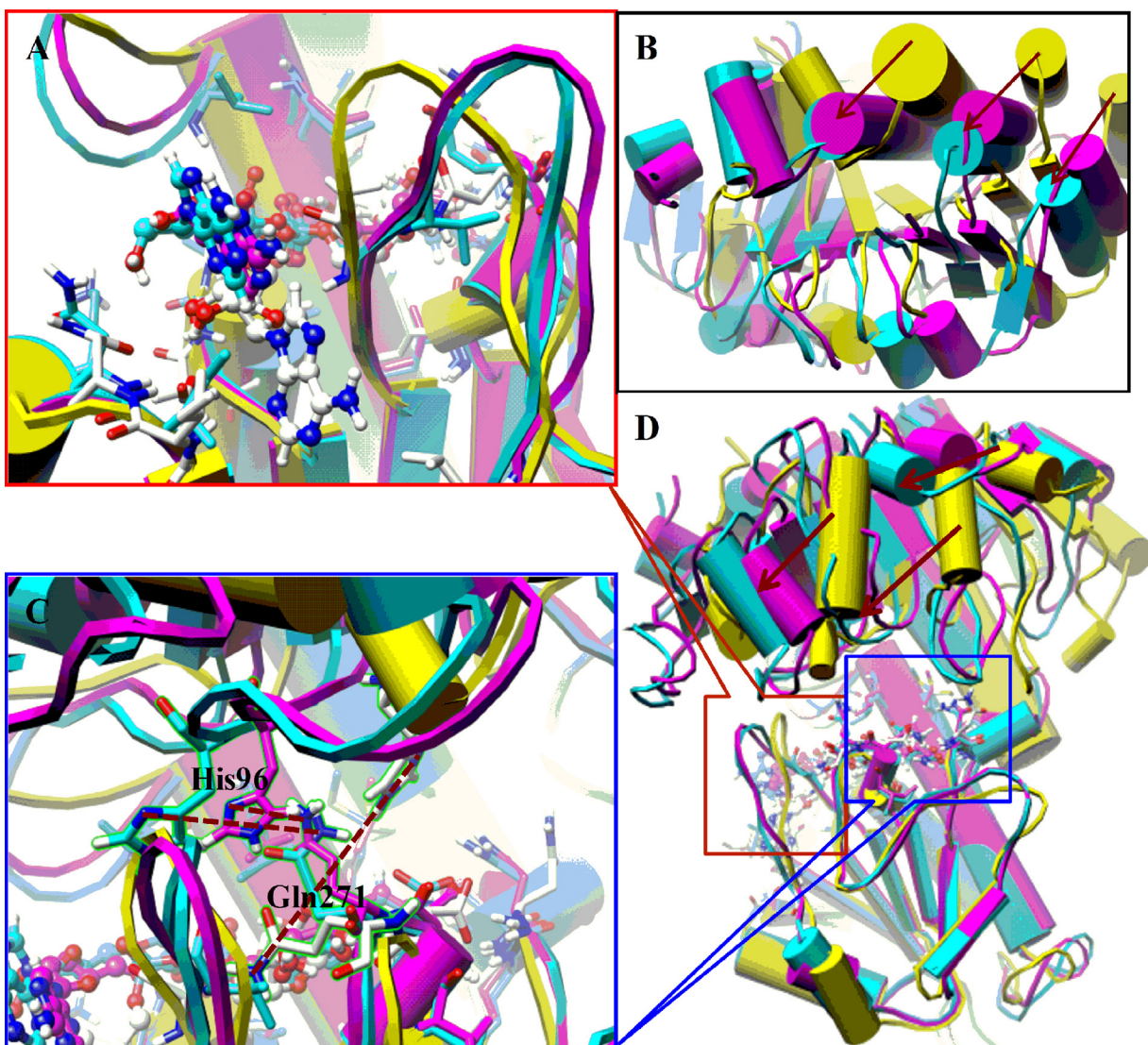


Fig. 9. Superimposition of the crystal structure and average structures from MD simulations for WT_hybrid (D). The crystal structure is colored in yellow, the average structures from 0–12 ns to 15–30 ns MD trajectories are in magenta and cyan, respectively. The protein is shown in pipes and planks, NADH is in ball and stick, and the surrounding residues are represented in sticks. The highlighted regions are shown in (A) and (C) insets, and top view of superimposition (B). The dark red arrow points the moving orientation of protein, and the dotted line represents the distance of His96ND1 and Gln271NE2. (For interpretation of the references to color in this figure legend, the reader is referred to the web version of this article.)

in future experiment, which maybe make the nicotinamide ring of NADH unstable and lead the protein to lose its activity. This finding perhaps provides helpful information for the design of new compounds targeting L-MtAlaDH. From the average structure in Fig. 8B, one can see that although Asp270 and the ribose of NADH cannot form stable hydrogen bonds, they are close to each other and the distances of heavy atoms fluctuate at 0.5 nm.

Likewise, for WT_holo system, the distance of OD1 of Asp270 and N7N of NADH still fluctuates at 0.4 nm, and other atomic distances between Asp270 and the ribose of NADH decrease before 8 ns, then they increase and fluctuate at 0.8 nm (see Fig. 8C). A hydrogen bond between N of Met301 and O7N of NADH is stabilized at 0.3 nm before 12 ns, afterwards it is broken. On the contrary, ND1 of His 96 and NE2 of Gln271 form a strong hydrogen bond after 5 ns. Average structure in Fig. 8D shows that the oxygen atoms of ribose are still close to Asp270 despite that the ribose slightly rotates. Compared with the major atomic distances in WT_hybrid, the hydrogen bond interactions in WT_hybrid tend to convert to those in WT_holo,

further verifying that NADH indeed induces the protein to change its conformation from open to closed state.

Altogether, the interactions between the ribose of NADH and Asp270 are weak, but Asp270 maintains the stability of nicotinamide ring of NADH mainly through hydrogen bond interactions. Additionally, Met301 plays an essential role in fixing the nicotinamide ring to prevent its rotation. His96 facilitates the protein converting its conformation from open state to closed state by interactions with Gln271.

3.4. Effect of single mutation on the structure and activity of L-MtAlaDH

The conserved residues His96 and Asp270 were mutated to investigate their effect on the structure and activity of protein. The time dependences of distances and the corresponding average structures for L-MtAlaDH with single mutation were shown in Fig. 10.

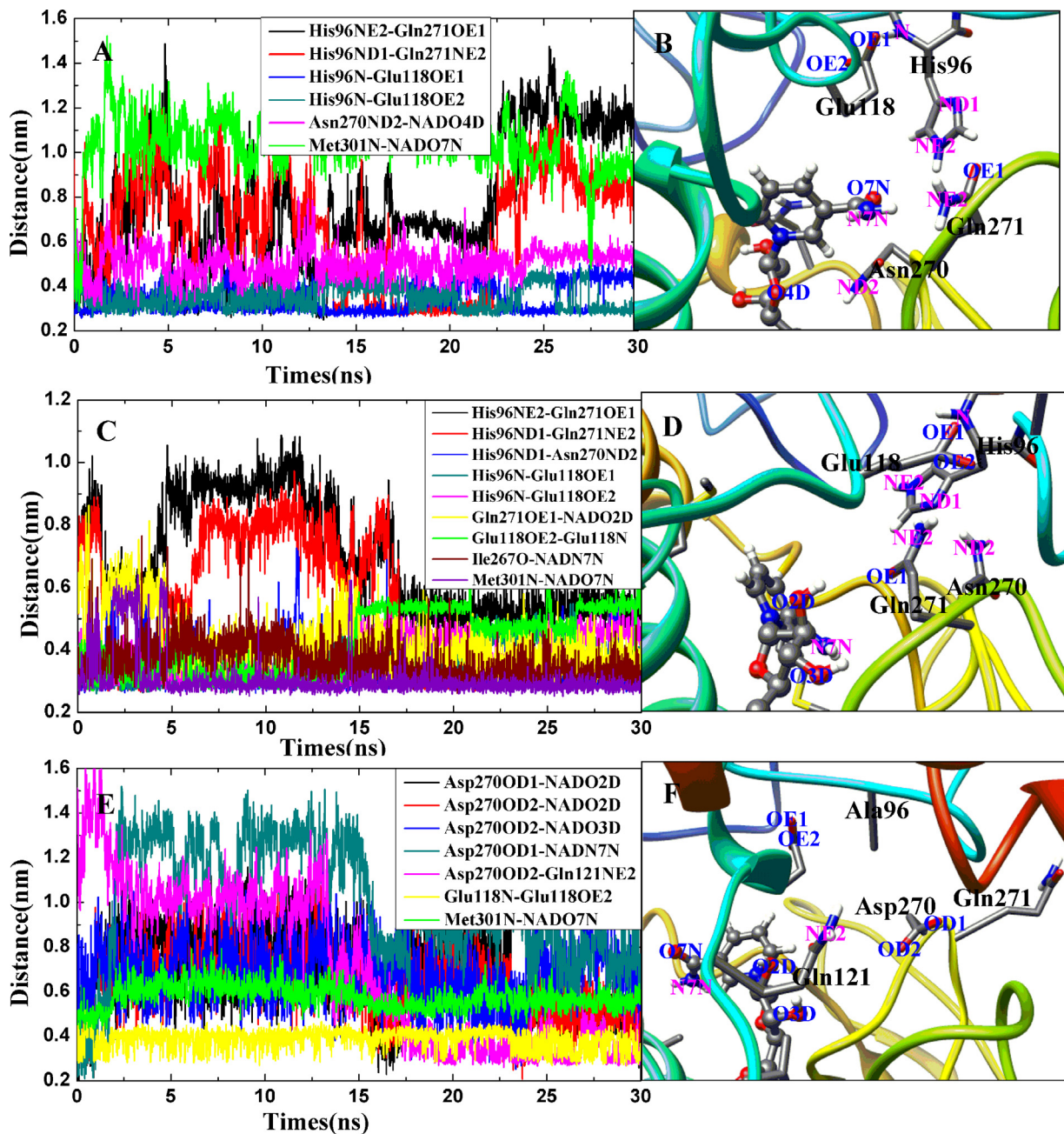


Fig. 10. Distance profiles between two heavy atoms and average structures from MD simulations, and for SM1.hybrid 0–17 ns trajectories were used. (A) and (B) for SM1.hybrid, (C) and (D) for SM2.crystal, (E) and (F) for SM3.hybrid.

For SM1.hybrid in Fig. 10A, the distance between His96 and Gln271 decreases, and ND1 of His96 forms a strong hydrogen bond interaction with NE2 of Gln271 from 13 ns to 22 ns, and then the bond is broken. This result shows that the D270N mutant leads to the disappearance of the original hydrogen bonds between Asp270 and the ribose of nicotinamide of NADH. Although the distance of ND2 of Asn270 with O4D of NADH maintains at 0.5 nm, the ribose rotates about 180° and changes its orientation (see Fig. 10B). Moreover, the hydrogen bond between N of Met301 and O7N of NADH disappears due to the rotation of nicotinamide ring. These results indicate that the protein changes its conformation from open state to closed state, but the nicotinamide ring and ribose would rotate owing to the lost of interactions between Asn270 and NADH, which leads to the structural rearrangement in active site,

and thus the distance between His96 and Gln271 increases from 22 ns.

From the data of SM2.crystal in Fig. 10C and D, one can see that the number and strength of hydrogen bonds in active site increase, but the hydrogen bond between Asn270 and NADH disappears, instead, a new strong hydrogen bond forms between ND2 of Asn270 and ND1 of His96. This indicates that Asn270 loses its interactions with NADH and sways to interact with His96. Meanwhile, the distance between His96 and Gln271 decreases to 0.5 nm and keeps stable after 17 ns due to the orientation change of Asn270, which results in the increase of distance of His 96 with Glu118. The distance between OE1 of Gln271 and O2D of NADH maintains at 0.4 nm from 5 ns, and that of N of Met301 with O7N of NADH is always stable at 0.3 nm. In addition, the distance of O of Ile267 with

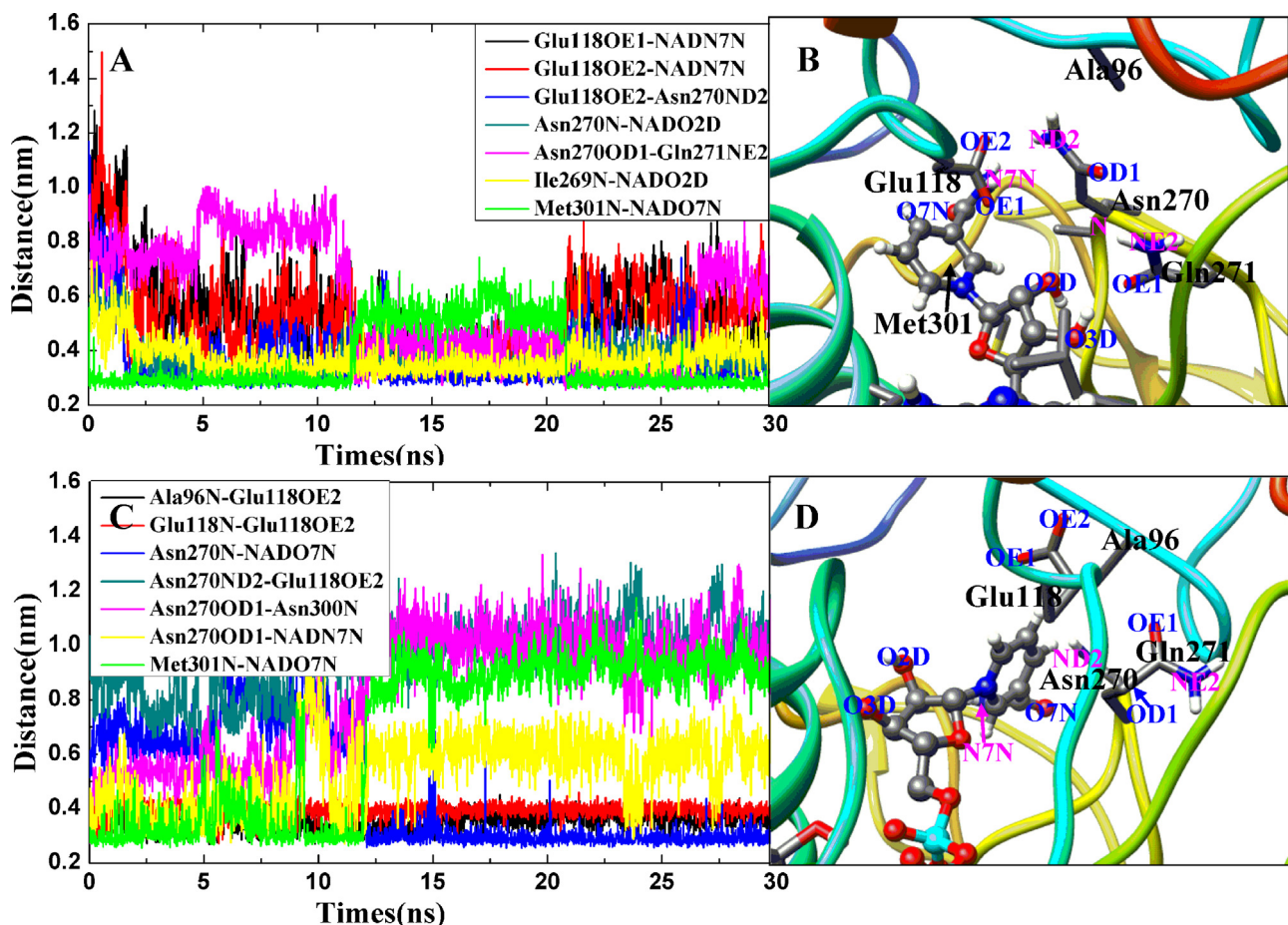


Fig. 11. Distance profiles between two heavy atoms of DM1_hybrid (A) and DM2_holo (C) systems. Average structures from 15 to 30 ns MD trajectories of DM1_hybrid (B) and DM2.holo (D) systems.

N7N of NADH fluctuates at 0.4 nm before 15 ns while it stabilizes at 0.35 nm after 15 ns. These results clearly indicate that the nicotinamide ring and ribose of NADH rotates slightly, and Asn270 and Gln271 exchange their orientations each other, however, Gln271 still tends to form stable interactions with His 96, further verifying that Asp270 plays an essential role in maintaining the stability of NADH, and His96 facilitates the protein converting its conformation through hydrogen bond interactions with Gln271.

Fig. 10E displays that there are few hydrogen bond interactions among these residues for SM3_hybrid. Although the distance of OD1 of Asp270 with N7N of NADH is about 0.3 nm at the beginning of simulations, it increases to 1.3 nm at 2 ns and fluctuates until 15 ns, then it decreases and maintains at 0.9 nm, which suggests that the interactions between Asp270 and the ribose of NADH disappear. However, OD2 of Asp270 forms a new strong hydrogen bond interaction with NE2 of Gln121 in substrate-binding domain from 18 ns, and the average structure in Fig. 10F clearly displays that Gln121 extends to interact with Asp270, but Gln271 is flipped out of the active site owing to the loss of interactions with Ala96. The results show that protein still converts its conformation from open state to closed state after His96 was mutated to Ala96, whereas Asp270 converts its interactions from NADH to Gln121, and Gln271 is flipped out of active site with H96A mutation.

In summary, whether the residue 96 or 270 is mutated, the protein always changes its conformations from open state to closed state upon binding NADH. However, the nicotinamide ring and ribose of NADH is unstable due to the loss of interactions of NADH with Asp270, and the structural rearrangement of active site leads

to the orientation change of Asn270 and Gln271, which makes the protein lose its activity.

3.5. Effect of double mutation on the structure and activity of L-MtAlaDH

We used the same method to investigate the effect of double mutation on the structure and activity of L-MtAlaDH. The distance profiles of possible hydrogen bonds and average structures are given in Fig. 11.

For DM1_hybrid in Fig. 11A and B, Glu118 gradually interacts with Asn270 and the nicotinamide ring of NADH with the conformational changes of protein, which indicates that the protein can still change its conformation from open state to closed state, but Asn270 loses the interactions of NADH and changes its orientation. The hydrogen bond of N of Met301 with O7N of NADH is very stable and strong unless N7N of NADH forms strong interactions with oxygen atoms of Glu118. Moreover, the distance of O2D of NADH with N of Ile269 stabilizes at 0.35 nm after 5 ns due to the loss of interactions of ribose with Asn270, which shows that Ile269 instead of Met301 fixes the ribose and prevents its rotation. In general, the protein still converts its conformation with double mutation, but double mutation brings a series of structural rearrangement and the loss of interactions in active site, which leads the protein to lose its catalytic activity.

Fig. 11C and D shows the distance deviation profiles between two heavy atoms and average structure for DM2_holo. It can be seen that the distance of N of Asn270 with O7N of NAD decreases

suddenly from 0.7 nm to 0.3 nm at 12 ns, which results in the increase of a series of distances of heavy atoms including Asn270ND2 with Glu118OE2, Asn270OD1 with Asn300N, Asn270OD1 with NADN7N, and Met301N with NADO7N. Compared with Fig. 11B, Fig. 11D shows a notable difference that the rotations of the ribose and nicotinamide ring of NADH lead to nicotinamide ring perpendicular to the original plane, and the hydrogen bonds of NADH with surrounding residues are disrupted.

These results suggest that the protein with double mutation can still convert its conformation from open state to closed state. However, the key interactions between NADH and Asn270 would disappear with mutation, consequently the structural rearrangement occurs and causes the loss of protein activity.

4. Conclusions

Based on the several mutation models, we have performed MD simulations and ED analysis to investigate the role of two conserved residues in wild type protein in the catalytic reaction. The results of ED analysis indicate that there are notable differences in the motion and conformational spaces of protein despite a considerable overlap. The results of MD simulations show that the protein still changes conformations from open state to closed state whether either or both of the two residues are mutated in active site, in other words, the presence of coenzyme NADH indeed induces the protein to convert its conformations. However, when the conserved residues were mutated, the nicotinamide ring and ribose of NADH would rotate with the loss of interactions of NADH with Asp270, and Gln271 loses the interactions with His96 in another domain and is flipped out of the active site. Simultaneously, the structural rearrangement causes the residues 270 to change its orientation and tend to interact with the residue in another domain, such as Gln121 or Glu118. Thereby, a series of sequential structural rearrangement in active site takes place to make the residues locate in unsuitable positions and lose the activity of protein. In conclusion, Asp270 maintains the stability of nicotinamide ring and ribose of NADH through hydrogen bond interactions, and His96 facilitates the protein converting its conformation from open state to closed state by interactions with Gln271. In addition, Met301 plays a critical role in fixing the nicotinamide ring of NADH to prevent its rotation.

Acknowledgement

This work was supported by National Natural Science Foundation of China (21173216, 31200048) and the Research Award Foundation for outstanding young scientist of Shandong Province (BS2013SW028). Special thanks also go to the Scientific Research Startup Funds (20100205), the School Youth Funds (XJ201211, XJ201214) and the Laboratory Open Fund (2013SK004) of Qufu Normal University for their funding.

References

- [1] B.R. Bloom, R.D. McKinney, The death and resurrection of tuberculosis, *Nat. Med.* 5 (1999) 872–874.
- [2] L.G. Wayne, H.A. Sramek, Metronidazole is bactericidal to dormant cells of *Mycobacterium tuberculosis*, *Antimicrob. Agents Chemother.* 38 (1994) 2054–2058.
- [3] R. Schnell, G. Schneider, Structural enzymology of sulphur metabolism in *Mycobacterium tuberculosis*, *Biochem. Biophys. Res. Commun.* 396 (2010) 33–38.
- [4] K.J. Siranosian, K. Ireton, A.D. Grossman, Alanine dehydrogenase (*ald*) is required for normal sporulation in *Bacillus subtilis*, *J. Bacteriol.* 175 (1993) 3796–3799.
- [5] Å.B. Andersen, P. Andersen, L. Ljungqvist, Structure and function of a 40000-molecular-weight protein antigen of *Mycobacterium tuberculosis*, *Infect. Immun.* 60 (1992) 2317–2323.
- [6] S.M. Tripathi, R. Ramachandran, Crystal structure of the *Mycobacterium tuberculosis* secretory antigen alanine dehydrogenase (Rv2780) in apo and ternary complex forms captures “open” and “closed” enzyme conformations, *Proteins* 72 (2008) 1089–1095.
- [7] J. Starck, G. Källenius, B. Marklund, D.I. Andersson, T. Åkerlund, Comparative proteome analysis of *Mycobacterium tuberculosis* grown under aerobic and anaerobic conditions, *Microbiology* 150 (2004) 3821–3829.
- [8] D. Ågren, M. Stehr, C.L. Berthold, S. Kapoor, W. Oehlmann, M. Singh, G. Schneider, Three-dimensional structures of Apo- and holo-L-alanine-dehydrogenase from *Mycobacterium tuberculosis* reveal conformational changes upon binding coenzyme binding, *J. Mol. Biol.* 377 (2008) 1161–1173.
- [9] B.P. Ling, M. Sun, S.W. Bi, Z.H. Jing, Y.J. Liu, Molecular dynamics simulations of the coenzyme induced conformational changes of *Mycobacterium tuberculosis* L-alanine dehydrogenase, *J. Mol. Graph. Model.* 35 (2012) 1–10.
- [10] W. Humphrey, A. Dalke, K. Schulten, VMD: visual molecular dynamics, *J. Mol. Graph.* 14 (1996) 33–38.
- [11] H.J.C. Berendsen, J.P.M. Postma, W.F. van Gunsteren, J. Hermans, *Interaction Models for Water in Relation to Protein Hydration*, Reidel, Dordrecht, 1981, pp. 331–342.
- [12] H.J.C. Berendsen, J.P.M. Postma, W.F. van Gunsteren, A. DiNola, J.R. Haak, Molecular dynamics with coupling to an external bath, *J. Chem. Phys.* 81 (1984) 3684–3690.
- [13] B. Hess, H. Bekker, H.J.C. Berendsen, J.E.M. Fraaije, LINCS: a linear constraint solver for molecular interactions, *J. Comput. Chem.* 18 (1997) 1463–1472.
- [14] T. Darden, D. York, L. Pedersen, Particle mesh Ewald. An $N \log(N)$ method for Ewald sums in large systems, *J. Chem. Phys.* 98 (1993) 10089–10092.
- [15] W. Humphrey, A. Dalke, K. Schulten, VMD – visual molecular dynamics, *J. Mol. Graph.* 14 (1996) 33–38.
- [16] C. Oostenbrink, A. Villa, A.E. Mark, W.F. van Gunsteren, A biomolecular force field based on the free enthalpy of hydration and solvation: the GROMOS force-field parameter sets 53A5 and 53A6, *J. Comput. Chem.* 25 (2004) 1657–1676.
- [17] D. van der Spoel, E. Lindahl, B. Hess, A.R. van Buuren, E. Apol, P.J. Meulenhoff, D.P. Tieleman, A.L.T.M. Sijbers, K.A. Feenstra, R. van Drunen, H.J.C. Berendsen, Gromacs User Manual version 4.0, 2005, www.gromacs.org
- [18] D. van der Spoel, E. Lindahl, B. Hess, G. Groenhof, A.E. Mark, H.J.C. Berendsen, GROMACS: fast, flexible and free, *J. Comput. Chem.* 26 (2005) 1701–1718.
- [19] J.L. Klepeis, K. Lindorff-Larsen, R.O. Dror, D.E. Shaw, Long-timescale molecular dynamics simulations of protein structure and function, *Curr. Opin. Struct. Biol.* 19 (2009) 120–127.
- [20] J. Zhang, Y. Xu, J. Shen, X. Luo, J. Chen, K. Chen, W. Zhu, H. Jiang, Dynamics mechanism for the autophosphorylation of CheA histidine kinase: molecular dynamics simulations, *J. Am. Chem. Soc.* 127 (2005) 11709–11719.
- [21] S. Hayward, A. Kitao, Molecular dynamics simulations of NAD⁺-induced domain closure in horse liver alcohol dehydrogenase, *Biophys. J.* 91 (2006) 1823–1831.
- [22] D.K. Chakravorty, S. Hammes-Schiffer, Impact of mutation on proton transfer reactions in ketosteroid isomerase: insights from molecular dynamics simulations, *J. Am. Chem. Soc.* 132 (2010) 7549–7555.
- [23] H. Fukunishi, H. Yagi, K. Kamijo, J. Shimada, Role of a mutated residue at the entrance of the substrate access channel in cytochrome P450 engineered for vitamin D3 hydroxylation activity, *Biochemistry* 50 (2011) 8302–8310.
- [24] F. Collu, A.V. Vargiu, J. Dreier, M. Cascella, P. Ruggerone, Recognition of imipenem and meropenem by the RND-transporter MexB studied by computer simulations, *J. Am. Chem. Soc.* 134 (2012) 19146–19158.
- [25] E.F. Pettersen, T.D. Goddard, C.C. Huang, G.S. Couch, D.M. Greenblatt, E.C. Meng, T.E. Ferrin, UCSF chimera – a visualization system for exploratory research and analysis, *J. Comput. Chem.* 25 (2004) 1605–1612.
- [26] H.J.C. Berendsen, S. Hayward, Collective protein dynamics in relation to function, *Curr. Opin. Struct. Biol.* 10 (2000) 165–169.
- [27] K. Natarajan, S. Senapati, Probing the conformational flexibility of monomeric FtsZ in GTP-bound, GDP-bound, and nucleotide-free states, *Biochemistry* 52 (2013) 3543–3551.
- [28] A. Amadei, A.B.M. Linssen, H.J.C. Berendsen, Essential dynamics of proteins, *Proteins* 17 (1993) 412–425.
- [29] D.M.F. van Aalten, A. Amadei, A.B.M. Linssen, V.G.H. Eijlsink, G. Vriend, H.J.C. Berendsen, The essential dynamics of thermolysin: conformation of the hinge-bending motion and comparison of simulations in vacuum and water, *Proteins* 22 (1995) 45–54.
- [30] D.M.F. van Aalten, J.B.C. Findlay, A. Amadei, H.J.C. Berendsen, Essential dynamics of the cellular retinol-binding protein evidence for ligand-induced conformational changes, *Protein Eng.* 8 (1995) 1129–1136.